Intermolecular Structure in a Polymer Glass: Electronic Excitation Transfer Studies

A. H. Marcus, Nathan A. Diachun, and M. D. Fayer*

Department of Chemistry, Stanford University, Stanford, California 94305

Received November 19, 1992; Revised Manuscript Received February 26, 1993

ABSTRACT: Electronic excitation transport among interacting polymer molecules lightly tagged with chromophore substituents is examined as a function of tagged polymer concentration in the polymeric solid. The technique of time-correlated single photon counting is employed to obtain time-resolved fluorescence depolarization data on solid mixtures of poly(methyl methacrylate-*co*-2-vinylnaphthalene) in a poly(methyl methacrylate) host. The time-dependent fluorescence anisotropy, the energy transport observable, is compared to a theory developed to model this system. The theory is based on a first-order cumulant approximation to the transport master equation. The model makes use of the Flory "ideality" postulate by depicting the intramolecular segmental distribution as a Gaussian with a second moment that scales linearly with chain size. At low copolymer concentration, the dynamics of excitation transfer depend only on intramolecular structure. At high copolymer concentration, excitation transfer occurs among chromophores on different copolymers in addition to intramolecular transfer. The only adjustable parameter in the treatment is the form of the intermolecular radial distribution function, $g(r)$. The sensitivity of the model is analyzed with respect to the behavior of $g(r)$. The theoretical treatment provides a quantitative description of the time and concentration dependence of the excitation transfer for the case of $g(r) = 1$ when $r \geq 20$ Å.

I. Introduction

The elucidation of intermolecular structure in dense polymer fluids and solid glasses is an unresolved topic that has stimulated numerous theoretical and experimental investigations.[1-12] There are many aspects to this problem. For example, the degree of interpenetration among neighboring polymer coils may be extensive, leading to random packing of the polymer segments.[13] In this case, the pair distribution function, $g(R_S)$, which represents the relative probability that the centers of gravity of two polymer molecules are separated by the distance R_S, is a constant (unity) for all separations. Alternatively, certain systems exhibit behavior where regions near the centers of gravity of Gaussian coils exclude segments belonging to other molecules. In such a situation, the pair distribution function is small for values of R_S similar to the radius of gyration (R_g), but asymptotically approaches unity as R_S increases. This deficit in radial distribution probability is referred to in the literature as a correlation hole.[8]

Knowledge of intermolecular polymer structure can be further applied to problems that focus on polymer blend morphology. The structure of microphase separated domains in polymeric mixtures is not well understood. A microdomain is a region where the segments of as few as two or three molecules of one component have aggregated. It has been shown that microdomains exist at temperatures well below the critical point in solid blends which appear macroscopically homogeneous.[14,15] The structure of these domains can directly affect the behavior of the glass transition temperature, since processes responsible for T_g are associated with distance scales comparable to domain size. Independent measurements of T_g and microdomain structure can therefore establish detailed characteristics such as the critical distance associated with the glass transition.[16]

Kinetic studies of polymer phase transitions can benefit from a detailed analysis of intermolecular structure. Phase separation in miscible polymer blends can be induced by variations in temperature, pressure, or composition. The final, equilibrium state contains different macroscopic regions (phases) dominated by different components of the blend. During the initial and intermediate stages of the phase transition, the structure, local concentration, and size of the microdomains present must evolve toward the final state. By following the trajectory of the microdomain structure, new insight can be gained concerning the mechanisms of polymer phase transitions.

In this paper, we report theoretical and experimental methods developed to study intermolecular structure in a polymeric glass. Measurements of electronic excitation transport (EET) among pendant chromophores randomly tagged to the backbone of a polymer coil in low concentration are employed to determine the proximity of other tagged coils. The energy transport occurs by the Förster mechanism, based on the dipolar coupling between an excited donor molecule and an unexcited (but otherwise identical) acceptor molecule. Because the transfer rates depend on interchromophore distance and orientation, the EET observable is extremely sensitive to the chromophore distribution. An analysis that combines these measurements with an appropriate theory provides the necessary information to describe the macromolecular structure.

Until recently, past research has focused on the characterization of intramolecular structure. For example, the effective radius of octadecylrhodamine B (ODRB) chromophores distributed on the surfaces of isolated triton X-100 micelles has been determined and found to agree with independent light scattering measurements of the micelle hydrodynamic volume.[17] Similarly, the root mean square radius of gyration of poly(methyl methacrylate-*co*-2-vinylnaphthalene) isolated in a poly(methyl methacrylate) matrix has been found to agree with light scattering measurements.[18] Both the micelle and the tagged copolymer cited above are clustered systems of chromophores. In the work of Ediger et al. and Peterson et al. the micelle or polymer concentration is low enough that the interaction between chromophores on neighboring clusters is negligible. As the concentration is increased, however, transfer of excitations between clusters may compete with intracluster transfer events. The combined contribution of intra- and intercluster excitation transfer causes the overall rate of the EET to increase. The excited-state dynamics that occur in the intermediate- and high-concentration limits for the ODRB/triton X-100 micelle

0024-9297/93/2226-3041$04.00/0

systems have been analyzed in a recent publication.[19]

In this work, we examine the intercluster EET among the chromophore substituents of a random copolymer. The copolymer is 6% atactic poly(methyl methacrylate-*co*-2-vinylnaphthalene) (P2VN–MMA). The vinylnaphthalene subunits serve as probe molecules that can be optically excited to an electronic singlet state. This copolymer is introduced into an atactic poly(methyl methacrylate) (PMMA) matrix which is optically inert. The excitation transfer is then measured as a function of copolymer concentration using the fluorescence detection technique of time-correlated single photon counting. The experimental results are compared to theoretical predictions previously developed to model clustered systems.[20]

The behavior of interacting clusters of chromophores can be understood as a superposition of processes which include both the internal dynamics of a single cluster and the external dynamics among cluster pairs. Thus, the survival probability of an excited chromophore will depend on the relative efficiency between competing high-frequency transfer processes (those which occur among chromophores in the same cluster) and lower frequency events (intercluster transfer) which increase in frequency and amplitude as the average cluster separation decreases. We adopt a formalism which makes use of a truncated cumulant approximation to the Green's function solution of the Pauli master equation.[21,22] The time-dependent motion of an excitation within an ensemble of interacting chromophores can be characterized by the function $G^S(t)$.[23,24] $G^S(t)$ is the diagonal portion of the Green's function. It represents the probability that the initially excited chromophore is still excited at some later time. $G^S(t)$ includes transfer events in which the excitation leaves the initial site and later returns but does not include the excited-state lifetime.

The usefulness of $G^S(t)$ lies in its relationship to the observable obtained from fluorescence depolarization experiments. A polarized excitation of an ensemble of randomly oriented chromophores results in a photoselective excited state. Only chromophores with the appropriate transition dipole vectors can be initially excited. Transfer of the excitation to surrounding molecules, which are randomly oriented, and subsequent emission by the excited molecule leads to depolarization of the observed fluorescence. This results in fluorescence anisotropies dominated by $G^S(t)$, provided other depolarization processes (such as chromophore rotation) occur on a slower time scale. For the experiments presented here, we obtain high-resolution excited-state decay profiles polarized both parallel and perpendicular to the excitation polarization. These decays are converted to fluorescence anisotropies which are related to $G^S(t)$ for the polymer system. The most significant result is that the concentration-dependent data can be reproduced with *no adjustable parameters* in the absence of a correlation hole. The maximum size of a correlation hole, which is consistent with the data, is determined.

This paper is organized in the following manner: In section II, we briefly discuss the application of the two-particle cumulant approximation to calculate the observables obtained from (P2VN–MMA)/(PMMA) systems. A general treatment of this problem has been reported previously.[20] Section III describes the experimental instrumentation and the preparative techniques employed. Section IV is a discussion of the results.

II. Theory and Calculation of Observables

In this section, we present a model for energy transport among identical chromophores randomly tagged to the backbones of polymer coils in the amorphous bulk state. The model is based on a truncated cumulant expansion as an approximation to the transport master equation. The cumulant is truncated at first order. Therefore, all transfer events between chromophores are due to pairwise interactions. Approximations of this type display excellent agreement with more accurate representations of the Green's function for infinite isotropic systems as well as restricted finite volume systems.[5,18,21,22,25] The first-order cumulant approximation provides a mathematically tractable approach for the complex problem examined here. The technique applied here is referred to as the "effective chromophore method".

We describe the excitation dynamics in polymer systems by separating $G^S(t)$ into two contributions, $G^S_{on}(t)$ and $G^S_{off}(t)$.[20] $G^S_{on}(t)$ describes transport "on" the coil containing the originally excited chromophore. This part of the energy transport is internal to the coil, corresponding to the zeroth-order term of a cumulant in coil density. $G^S_{off}(t)$ describes forward and back transfer from the originally excited coil to chromophores on neighboring coils. This part of G^S represents an interaction between coil pairs and corresponds to the first-order term of the cumulant. In the context of this model, all transfer events are independent. That is, the probability of transfer to other coils is unaffected by the probability of transfer within a coil. According to standard methods of probability theory,[20,26] this implies that the ensemble average decay of the Green's function can be written $\langle G^S(t)\rangle = \langle G^S_{on}(t)\rangle\langle G^S_{off}(t)\rangle$. Thus, in the limiting case of this approximation, the observed excitation transfer in a concentrated tagged polymer system can be viewed as the low-concentration dynamics (isolated coils) modified by the dynamics due to intercoil interactions. We are then faced with the separate problems of calculating $\langle G^S_{on}(t)\rangle$ and $\langle G^S_{off}(t)\rangle$.

A. Microsystem Calculations: Chromophores Distributed within two Gaussian Surfaces. Consider two identical polymer coils with radius of gyration R_g, separated by the distance R_S (Figure 1). Both coils have chromophores randomly oriented and distributed along their backbones. One is designated the "donor coil" while the other is the "acceptor coil". The intercoil separation may be large as illustrated in Figure 1a, or R_S may be small so that the segments interpenetrate extensively (Figure 1b). We examine the case where a single chromophore on the donor coil is excited and incoherent energy transfer to surrounding unexcited chromophores can occur by a dipole–dipole type mechanism.[27]

In general, the ensemble average decay of excitation probability of a donor molecule surrounded by a distribution of acceptors is given by[20,28]

$$\ln\langle G^S(t)\rangle = -\frac{\rho}{2}\int_{space}\{1-\exp[(-2t/\tau)(R_0/|\mathbf{r}|)^6]\}u_a(\mathbf{r})\,d\mathbf{r} \tag{2.1}$$

Here, "donor" means the initially excited molecule, while "acceptors" refer to unexcited but otherwise identical molecules. In eq 2.1, ρ represents the number density of acceptor molecules, τ is the excited-state lifetime, R_0 is the characteristic Förster transfer distance, and $\mathbf{r}$ is the vector which spans the volume of the chromophore distribution. The vector distribution $u_a(\mathbf{r})$ is defined such that $\rho u_a(\mathbf{r})\,d\mathbf{r}$ is the number of acceptors in the region between $\mathbf{r}$ and $\mathbf{r}+d\mathbf{r}$. The normalization condition is

$$\rho\int_{space}u_a(\mathbf{r})\,d\mathbf{r} = N-1 \tag{2.2}$$

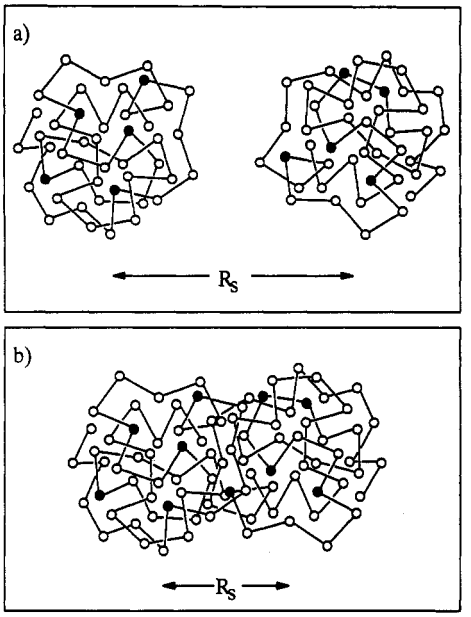

Figure 1. Schematic representation of two polymer molecular separated by a distance R_S. Both molecules are characterized by the radius of gyration, R_g. The open circles represent optically inert subunits while the closed circles represent the naphthalene-tagged sites where an excitation may reside. The degree of interpenetration of the segments belonging to the two molecules depends on the relative size of R_S in comparison to $2R_g$. For $R_S > 2R_g$ as shown in (a), there is little interpenetration. For $R_S < 2R_g$ as shown in (b), there is extensive interpenetration.

where N is the total number of chromophores (donor and acceptors) within the finite volume. The integrals in eqs 2.1 and 2.2 are carried over the space containing the donor and acceptor chromophores.

Equation 2.1 describes the excitation decay of a single donor molecule on the donor coil interacting with a distribution of chromophores on the acceptor coil. Since the distribution of acceptor chromophores depends on the location of the original donor position, eq 2.1 must be averaged over the space of the donor coil.

$$\langle G^S(t)\rangle = \frac{1}{V_d}\int_{space}\langle G^S(t,\mathbf{r}_d)\rangle u_d(\mathbf{r}_d)\,d\mathbf{r}_d \quad (2.3a)$$

$$\langle G^S(t,\mathbf{r}_d)\rangle = \exp\left(-\frac{N-1}{2V_a}\int_{space}\{1-\exp[(-2t/\tau)(R_0/|\mathbf{r}_{ad}|)^6]\}u_a(\mathbf{r}_a)\,d\mathbf{r}_a\right) \quad (2.3b)$$

In eqs 2.3 the volumes V_d and V_a are those occupied by the donor and acceptor distributions. The vector $\mathbf{r}_{ad}$ joins the positions of the acceptor and donor molecules.

To perform the integrals in eqs 2.3, we adopt a multiframe coordinate system. The space containing the donor and acceptor distributions is spanned by the vectors $\mathbf{r}_1$ and $\mathbf{r}_2$, respectively. The donor–acceptor separations are then given by a coordinate transformation[20] that depends on the distance between the coil centers of gravity. Thus, $\mathbf{r}_2 = A\mathbf{r}_{12}'$, where $\mathbf{r}_{12}'$ spans the space containing the acceptor molecules in a newly defined coordinate system. The donor and acceptor distributions are modeled as Gaussian functions after the Gaussian chain model:[29]

$$u_d(\mathbf{r}_1) = \left(\frac{3}{2\pi\langle R_g^2\rangle}\right)\exp\left(\frac{-3}{2\langle R_g^2\rangle}r_1^2\right),$$
$$d\mathbf{r}_1 = r_1^2\sin\theta_1\,dr_1\,d\theta_1\,d\phi_1 \quad (2.4a)$$

$$u_a(\mathbf{r}_2) = \left(\frac{3}{2\pi\langle R_g^2\rangle}\right)\exp\left(\frac{-3}{2\langle R_g^2\rangle}r_2^2\right),$$
$$d\mathbf{r}_2 = r_2^2\sin\theta_2\,dr_2\,d\theta_2\,d\phi_2 \quad (2.4b)$$

Substitution of eqs 2.4 into eqs 2.3 and further simplification by symmetry arguments result in

$$\langle G^S_{off}(t,R_S)\rangle = 2\pi\left(\frac{3}{2\pi\langle R_g^2\rangle}\right)^{3/2}\int_{r_1}\int_{\theta_1}G^S(r_1,\theta_1)\times\exp\left(\frac{-3}{2\langle R_g^2\rangle}r_1^2\right)\sin\theta_1\,dr_1\,d\theta_1 \quad (2.5a)$$

$$\ln[G^S(r_1,\theta_1)] = (N-1)\pi\left(\frac{3}{2\pi\langle R_g^2\rangle}\right)^{3/2}\times\int_{r_2}\int_{\theta_2}\{\exp[(-2t/\tau)(R_0/r_{12}'(\theta_1,\theta_2,r_1,r_2))^6]-1\}\times\exp\left(\frac{-3}{2\langle R_g^2\rangle}r_2^2\right)r_2^2\sin\theta_2\,dr_2\,d\theta_2 \quad (2.5b)$$

where

$$|r_{12}'(\theta_1,\theta_2,r_1,r_2)|^2 = r_1^2 + r_2^2 + 2R_S[r_2\cos\theta_2 - r_1\cos\theta_1] - 2r_1r_2\cos(\theta_2-\theta_1) + R_S^2 \quad (2.5c)$$

Equations 2.5 express the excitation dynamics between two coils separated by the distance R_S. In the limit of vanishingly small R_S the donor and acceptor distributions superimpose and the resulting excitation dynamics occur on a single isolated coil. That is, $\langle G^S(t,0)\rangle = \langle G^S_{on}(t)\rangle$. For all finite separations, these integrals must be evaluated numerically.

Thus far, we have derived $\langle G^S(t)\rangle$ for two specific cases: $\langle G^S_{on}(t)\rangle$ describes excitation transfer among N chromophores on a single isolated coil, while $\langle G^S_{off}(t,R_S)\rangle$ (eqs 2.5) describe excitation transfer between a donor chromophore on a "donor coil" and $N-1$ acceptor chromophores on an "acceptor coil", separated by the distance R_S. $\langle G^S_{off}(t,R_S)\rangle$ contains the details of the chromophore distributions and it represents the configurational average of the transport dynamics due to the pairwise interaction between two coils. This step reduces the calculation to the equivalent of transfer between two "effective chromophores". The internal structure of the chromophore clusters is contained in the calculation of $\langle G^S_{off}(t,R_S)\rangle$. These two descriptions of the coil transport dynamics, which separately contain internal and pairwise interactions, are sufficient to model the copolymer concentration dependence of G^S.

B. Calculations for Tagged Copolymers in Solid Solution. An extension of eqs 2.5 to experimental observables must consider the effect of molecular interactions on both the intramolecular structure and the intermolecular radial distribution function. A complete description of the bulk structure would include the complex interdependencies of the possible intra- and intermolecular conformations. This formidable task has been addressed over the years by several workers.[1,2,8,9,30-35] The problem is vastly simplified by making use of the well-established fact that individual coils in dense melts and glasses are ideal.[8,9] The concept of a Θ condition in condensed disordered states has been repeatedly verified in the literature.[35] In these situations, the forces which lead to intramolecular excluded volume are balanced by those forces arising from the interaction between molecules. The Flory postulate predicts that the segmental distribution of an ideal chain (Θ condition) is Gaussian for distances beyond a few statistical segment lengths with a second moment that scales linearly with the chain size.[13] Since

the chains in these experiments are *lightly* tagged with probe consitituents (less than one probe per statistical segment length), the average interchromophore separation is large enough for the energy transport observable to reflect the Gaussian chain structure. Furthermore, a previous study has shown that low tagging fractions do not perturb the chain structure.[14] Therefore, it is reasonable to assume an ideal Gaussian distribution for the individual coil configurations. We proceed by averaging eqs 2.5 over intermolecular radial separations relevant to the energy transport observable. Ideality approximations such as this one have been successfully applied to related theories of polymer structure including the rotational isomeric state model, the RPA calculations of de Gennes, and the RISM theory for dense cyclic polymer melts.[8,33,35] Curro and Schweizer have argued that since the intramolecular correlation function is a good approximation, the resulting intermolecular calculation (which in this work determines the energy transport observable) will be a reasonable approximation as well.

The thermodynamic limit of $\langle G^S_{off}(t,R_S)\rangle$ can be achieved by averaging over the coil pair separation, R_S, in the limit of infinite coil number and infinite volume. The ratio of coils to volume is restricted to equal the solution concentration.[36] It is straightforward to obtain a copolymer concentration dependent expression for $\langle G^S_{off}(t,R_S)\rangle$ which includes an average intermolecular radial distribution function, $g(R_S)$:

$$\ln\langle G^S_{off}(t,c)\rangle = -4\pi c\int_0^\infty [1-\langle G^S_{off}(t,R_S)\rangle]R_S^2 g(R_S)\,dR_S \tag{2.6}$$

where the concentration, c, is expressed as a volume fraction.

In eq 2.6, $g(R_S)\,dR_S$ represents the probability that the center of mass of a polymer molecule (modeled as a symmetric, Gaussian function) lies within the radial distance R_S and $R_S + dR_S$ from the reference coil's center of mass. Strictly speaking, a polymer intermolecular radial distribution function describes the relative probability of finding two sites on different chains separated by R_S, averaged over all possible combinations of interchain sites, averaged over all possible chain configurations. Since the ideal Gaussian coils are spherically symmetric, this amounts to the same thing as the interchain center to center pair distribution defined above.

The form of $g(R_S)$ serves to characterize the intermolecular polymer structure as a measure of the degree of interpenetration among neighboring chain segments. As stated previously, the bulk may be comprised of ideal coils with center of masses randomly located throughout the material. In this case, the intermolecular excluded volume only includes the "hard sphere" repulsions between chain segments. The radial distribution function then has values remarkably close to unity for distances greater than the length characterizing the chain thickness. Alternatively, some melt systems may exhibit density fluctuations that occur on longer length scales which extend out to the radius of gyration. Recent X-ray scattering investigation of polyethylene melts[2] in combination with a tractable theoretical model have measured radial distribution functions dominated by hard core segmental repulsion. The form of $g(R_S)$, in this case, was zero for distances less than 4.8 Å (the cross sectional contact distance in polyethylene) followed by an extremely rapid approach to unity. Since theoretical predictions for more complicated systems are not currently possible, the EET experiments in this work combined with eq 2.6 provide a useful means to probe the form of $g(R_S)$.

Table I. Physical Characteristics of the Guest (Poly(2-vinylnaphthalene-*co*-methyl methacrylate)) and Host (Poly(methyl methacrylate)) Polymers[a]

polymer	M_w	M_w/M_n	% 2-VN	$\langle N_{chrom}/coil\rangle$	N_{mon}	N_{stat}	$\langle R_g^2\rangle^{1/2}$/Å
guest	51 900	1.47	6.5	32	501	80.2	57.9
host	93 300	2.01	0	0	932	149	79.1

[a] M_w is the weight-average molecular weight, M_w/M_n is the polydispersity, % 2-VN is the number percent naphthyl subunits, $\langle N_{chrom}/coil\rangle$ is the average number of chromophores per molecule, N_{mon} is the number of monomers per molecule, N_{stat} is the number of statistical segments per molecule, and $\langle R_g^2\rangle^{1/2}$ is the rms radius of gyration based on the random coil model.

Equation 2.6 describes the decay of excitation probability in a concentrated tagged copolymer solution due solely to intercoil transfer events. The intracoil transfer, which is present at all concentrations, contributes to the overall decay according to $\langle G^S(t,c)\rangle = \langle G^S_{on}(t)\rangle\langle G^S_{off}(t,c)\rangle$.[20] According to eq 2.6, $\langle G^S_{off}(t,c)\rangle$ approaches unity as the coil concentration approaches zero. This allows the overall decay of G^S to approach $\langle G^S_{on}(t)\rangle$ with decreasing concentration as expected.

The function G^S represents the probability decay of a polarized excitation due to energy transfer. Its relationship to the fluorescence anisotropy, which contains all sources of depolarization, can be written as

$$r(t,c) = \langle \Phi(t)\langle G^S(t,c)\rangle\rangle \tag{2.7}$$

Here, $\Phi(t)$ contains processes besides energy transport which contribute to the depolarization. The most important of these is molecular reorientation, which occurs on a much slower time scale than the energy transport we wish to observe. The outside brackets in eq 2.7 indicate a configurational average that includes correlations between $\Phi(t)$ and the energy transport. The difference in time scales, however, suggests the correlations are insignificant and that molecular rotation is independent of the excitation transfer. Thus, eq 2.7 can be rewritten as

$$r(t,c) = \exp(-t/\tau_{rot})\langle G^S(t,c)\rangle \tag{2.8}$$

where τ_{rot} is the rotational correlation time.

III. Experimental Methods

A. Sample Preparation. A 6.5% copolymer of methyl methacrylate (MMA) and 2-vinylnaphthalene (2-VN) was prepared using the methods described by Peterson et al.[14] The fraction of 2-VN subunits in the copolymer was determined by measuring the absorbance of a known quantity of the material dissolved in CH_2Cl_2. The concentration of substituted naphthalene was determined based on the molar extinction coefficient for 2-ethylnaphthalene (350 M^{-1} cm^{-1} at 320 nm). This polydisperse material (M_w = 36 900, M_w/M_n = 2.16) was fractionated by size exclusion chromatography using a preparative gel permeation chromatograph (GPC) fitted with a Polymer Laboratories PLgel resin 500-Å column. Toluene was used as eluent. The molecular weights and polydispersities of the fractions were determined with a Waters Associates analytical GPC using THF as eluent.

The physical characteristics of the guest copolymer and the host polymer used in this study are reported in Table I. The host PMMA was purchased from Aldrich Chemical Co. It was further purified by reprecipitation in methanol two times. Samples were prepared by quantitatively mixing solutions of the guest copolymer and the host polymer in benzene. All weights were measured using a Gram-Attic balance (Fisher Scientific Co.) accurate to within ±0.0001 g. Volumes were measured with calibrated volumetric flasks and pipets.

The samples were made as consecutive dilutions of a concentrated sample. A stock solution of 15% host PMMA in benzene

Table II. Intercoil EET Samples[a]

vol %	τ/ns	width/μm	OD	vol %	τ/ns	width/μm	OD
20.0	47.2	40	0.2	2.5	50.5	300	0.19
10.0	48.6	80	0.2	3/8	49.0	1600	0.15
5.0	50.0	150	0.19	1/8	49.0	1600	0.05

[a] Vol % is the copolymer volume percent, τ is the measured radiative fluorescence lifetime, width is the sample thickness, and OD is the measured optical density at the absorption maximum (λ_{max} = 320 nm).

was prepared. An aliquot of this solution was combined with the guest copolymer to make a 20% guest/host mixture. Less concentrated samples (10, 5, 2.5, 0.375, and 0.125%) were made by consecutive dilution of the 20% solution. These polymer/benzene solutions were then freeze-dried by immersion in liquid nitrogen followed by sublimation of the frozen benzene under vacuum.

B. Experimental Techniques. Optical quality samples were obtained by compression molding the freeze-dried material above the glass transition temperature (T_g = 105 °C). The procedure was similar to that used by Ediger[15] and Peterson,[14] although there are some notable differences. The freeze-dried material was loaded into a Specac heatable die cell with polished stainless steel platens. This die cell was sealed in an aluminum bag which was subsequently purged with nitrogen gas. The bag and die cell were placed between the heated platens of a Carver die press. The temperature of the sample was monitored using a thermocouple inserted into the base of the die. After the sample temperature was held at 155 °C for 20 min, the die was pressed to 2.5 metric tons for 2 min. The die cell was immediately removed from the hot Carver press and quickly cooled with dry ice. All samples were made with sufficiently narrow width (see Table II) to ensure an optical density close to 0.2 at the peak absortpion wavelength (320 nm). The optical quality of the samples was checked using a polarizing microscope. The samples were found to be optically clear and free of birefrigence.

Absorption spectra of the samples were measured using a Hewlett-Packard 8452A diode array spectrophotometer. Time-resolved fluorescence spectra were measured using time-correlated single photon counting. The apparatus and technique are described in detail elsewhere.[18,37] The excitation pulses were provided by the cavity dumped output of a synchronously pumped dye laser tuned to 640 nm and frequency doubled to 320 nm. The pulse repetition rate was 823 kHz, the pulse duration was ~10 ps, and typical pulse energies, after doubling, were ~1 nJ. The excitation intensity was attenuated so that one fluorescent photon was detected for every 80 incident excitation pulses. Fluorescent photons were detected from the front face of the samples using a Hamamatsu microchannel plate in combination with a subtractive double monochromator tuned to 337 nm. The instrument response functions for this apparatus, although not symmetric, had full widths at half-maxima which varied between 40 and 56 ps.

Time-dependent decays of the polarized components of fluorescence, $I_{\parallel}(t)$ and $I_{\perp}(t)$, were collected in the following manner. A detection polarizer was held fixed while a Pockels cell was used to switch the plane polarization of the excitation beam between horizontal and vertical orientations. Each orientation was sampled for equal amounts of time, alternately changing the polarization direction every 20 s. This procedure minimized the effect of laser instabilities over long periods of time as well as any inherent bias in the detection system.

Data sets were collected for a time duration such that the peak of each decay contained approximately 45 000 counts. The fluorescence anisotropy was then calculated by point by point addition and subtraction of the fluorescence decays.

$$r(t) = \frac{I_{\parallel}(t) - I_{\perp}(t)}{I_{\parallel}(t) + 2I_{\perp}(t)} \tag{3.1}$$

C. Data Analyses. Theoretical anisotropies were calculated using eqs 2.5, 2.6, and 2.8 and directly compared to the data. The choice of time zero was made by matching the rising edge of both the data and the measured instrument response functions. The time corresponding to the peak of the instrument response (typically, 3/4 up the rising edge) was taken as time zero.

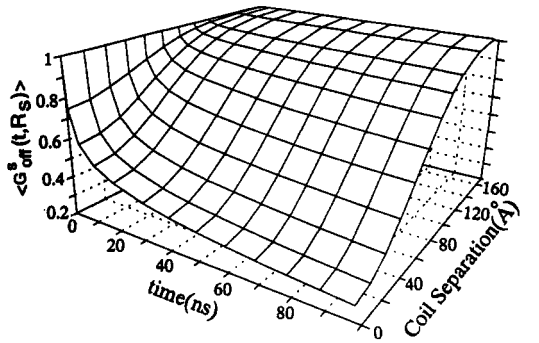

Figure 2. The Green's function solution, $\langle G^S_{off}(t,R_S)\rangle$, given by eqs 2.5 for two Gaussian correlated distributions of chromophores separated by the distance R_S. The values used for the radius of gyration, R_g, and the average number of chromophores per chain, N_{chrom}, are given in Table I. Most of the action of $\langle G^S_{off}(t,R_S)\rangle$ occurs within the range $R_S < 2R_g$.

IV. Results and Discussion

It is evident from eqs 2.5 that the only adjustable parameters in the cumulant approximation are the Förster critical transfer distance and the root mean square (rms) radius of gyration. The dynamic Förster distance for 2-ethylnaphthalene dispersed in PMMA was previously measured to be 13.0 ± 0.6 Å.[15] The orientationally dependent transfer distance is then obtained by multiplying the dynamic R_0 by the factor $(\gamma)^{1/3}$ (=0.8468) which includes geometrical considerations of the chromophore distribution.[14,28] The rms radius of gyration is determined from the molecular weight provided both the statistical segment length (l) and the number of statistical segments (N_{stat}) are known.

$$\langle R_g^2\rangle^{1/2} = N_{stat}^{1/2} l/6 \tag{4.1}$$

The number of statistical segments is obtained from the relation, $N_{stat}l = N_{mon}l_{mon}$, where N_{mon} and l_{mon} (≅2.54 Å) are the number of monomers and the monomer length, respectively. The statistical segment length for several copolymers of 2-VN and MMA with various molecular weights has been determined by Peterson et al.[14] This value (l = 15.9 Å) was established using EET measurements on isolated, tagged copolymers in bulk PMMA. It corresponds to radii of gyration identical to those obtained by light scattering measurements of polymer chains with identical molecular weights dissolved in Θ solvents. It has also been determined that for the low tagging used, l is not perturbed by the naphthyl tags.[14] Table I lists the rms radii of gyration for both the copolymer and the host based on this information.

Having reliable values for both the Förster transfer distance and the radius of gyration, we can calculate the copolymer concentration dependence of the EET for any radial distribution function *without recourse to adjustable parameters*. Figure 2 shows plots of $\langle G^S_{off}(t,R_S)\rangle$ obtained from eqs 2.5. (The value used for the lifetime is that obtained from the most dilute sample shown in Table II.) An important characteristic of this function is that most of its action occurs for coil separations less than twice the radius of gyration. Thus, we would expect the ensemble average of G^S determined by eq 2.6 to be most sensitive to values of $\langle G^S_{off}(t,R_S)\rangle$ for R_S in the range $R_S \leq 2R_g$. This means that the EET dynamics should be sensitive to the form of the radial distribution function in this range as well.

$\langle G^S_{off}(t,c)\rangle$ curves corresponding to the concentrations reported in Table II were constructed by numerically

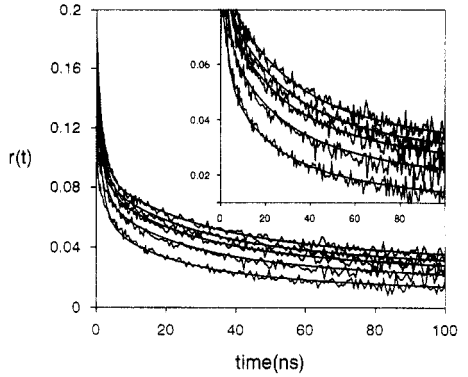

Figure 3. Time-dependent anisotropy decays and theoretical calculations for the P(2VN–MMA)/PMMA systems characterized by Tables I and II. For these calculations, the radial distribution function $g(R_S) = 1$ for all R_S. The lowest copolymer concentration (vol % = $^3/_8$%) decays the least and represents intramolecular energy transfer. Subsequently decreasing decays contain contributions from intermolecular energy transfer for copolymer concentrations 2.5, 5.0, 10, and 20%.

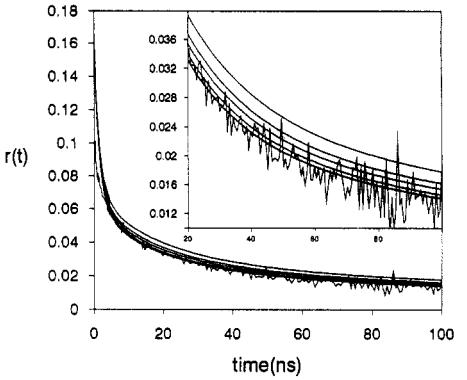

Figure 4. Comparison of experimental time-dependent anisotropy decay for the 20% sample with theoretical calculations based on hard shell $g(R_S)$ given by eq 4.4. The fastest theoretical decays are indistinguishable and correspond to σ = 0.0 and 11.6 Å. Subsequently slower decays correspond to σ = 29.0, 40.5, 46.3, and 57.9 Å.

integrating the intercoil decays, $\langle G^S_{off}(t,R_S)\rangle$, using eq 2.6. These in turn were used to make theoretical anisotropies according to

$$r(t,c) = r_{on}(t)\langle G^S_{off}(t,c)\rangle \qquad (4.2)$$

Here, $r_{on}(t)$ represents the experimentally determined fluorescence anisotropy due to depolarization processes that occur on isolated, noninteracting polymer coils. It contains the intracoil EET as well as contributions to the anisotropy from chromophore rotation. For analysis of isolated chain structure, $G^S_{on}(t)$ is calculated as described previously.[14] Since we are only interested in intercoil EET, for simplicity the measured anisotropy of the isolated coil was fit to a triexponential function,

$$r_{on}(t) = 0.0968\exp[-(t/1.67\text{ ns})] + 0.0469\exp[-(t/25.7\text{ ns})] + 0.043\exp[-(t/457\text{ ns})] \qquad (4.3)$$

Equation 4.3 provides a smooth curve for use in eq 4.2. The isolated coil data were obtained from the most dilute samples (c = $^3/_8$ and $^1/_8$%) listed in Table II. The anisotropies obtained from both of these low-concentration samples were identical, indicating that the dilute, intracoil EET limit had been achieved.

The fluorescence lifetimes of all the samples were determined from the total fluorescence, $I_{tot}(t) = I_{\parallel}(t) + 2I_{\perp}(t)$. These decays were monoexponential with radiative lifetimes listed in Table II. The independence of τ on concentration and the monoexponential form of $I_{tot}(t)$ indicate the absence of concentration-dependent processes such as excimer trapping or radiative reabsorption.

Figure 3 shows anisotropy decays and calculations for the intermediate- and high-concentration samples. For the calculations presented in this figure, the intermolecular radial distribution function $g(R_S) = 1$ for all R_S, corresponding to the absence of a "correlation hole". The intracoil decay (c = $^3/_8$%) is the slowest. The calculated line through these data is eq 4.3. The curves that lie below represent intercoil EET for concentrations c = 2.5, 5, 10, and 20%. As the coil concentration is increased, the rate of EET also increases. This shows that at these copolymer concentrations, intercoil EET is effectively competing with intracoil EET. The slight disagreement for the highest concentrations at very short time is due to a trace fluorescent impurity in the host PMMA. The fluorescence from this impurity occurs only at very short time and is detectable for the lowest concentration samples ($^3/_8$ and $^1/_8$%). This leads to a small inaccuracy of eq 4.3 at very short time which is amplified by eq 4.2. Despite this difficulty, the theoretical calculations, with *no adjustable parameters*, are in quantitative agreement with the data. The theory, based on a random distribution of ideal polymer coils, correctly predicts both the amplitude and the functional form of the anisotropy decays.

Although eq 2.8 fits the data exceptionally well, it is necessary to analyze the sensitivity of these calculations to the possible form of $g(R_S)$. Clearly, the assumption $g(R_S) = 1$ for all R_S is unrealistic for distances smaller than the characteristic chain segment diameter. A more reasonable form must include a cutoff representing the hard core interaction of individual segments followed by a rise to unity characterized by a characteristic length, λ. Since accurate theoretical predictions of $g(R_S)$ for all but the most simple chain systems are presently unavailable,[38] it is instructive to perform the above analyses using model correlation hole functions.

Recent investigations by Honnell and co-workers[2] of polyethylene melts suggest the dominant feature of $g(R_S)$ in this system is the monomeric hard core exclusion which depends on the cross sectional diameter of the chain. On the other hand, de Gennes' RPA calculations suggest the correlation hole may extend with appreciable depth as far as the radius of gyration. For simplicity, we choose to model these situations with the following distributions.

$$g(R_S) = H(R_S - \sigma) = 0, \quad \text{if } R_S \le \sigma$$
$$= 1, \quad \text{if } R_S > \sigma \qquad (4.4)$$

and

$$g(R_S) = 1 - e^{-(R_S - \sigma)/\lambda} \qquad (4.5)$$

The Heaviside step function, eq 4.4, contains a hard core excluded volume effect which turns on at the contact diameter, σ. A "softer" excluded volume that abruptly turns on at σ and then continues to climb toward unity can be simulated using eq 4.5. In this case, the "width" of the hole depends on both the contact distance, σ, and the characteristic length, λ.

Figure 4 shows comparisons of the 20% data with calculated anisotropies based on hard shell radial distributions given by eq 4.4. The values of σ are 0, 11.6, 29.0, 40.5, 46.3, and 57.9 Å. The fastest calculated decays correspond to the smallest contact distances. Increasing the magnitude of σ tends to slow the theoretical decays because the coils are prevented from interpenetrating to this extent. The calculations for σ = 0 and 11.6 Å are

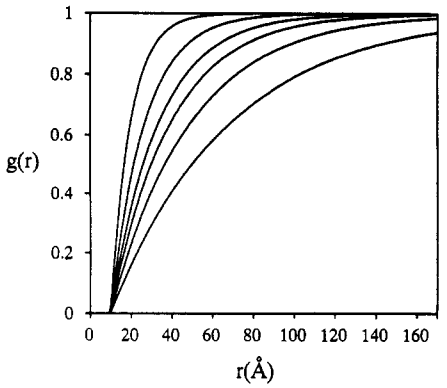

Figure 5. Plots of model radial distribution function given by eq 4.5. For all curves, σ = 10 Å. The values of λ correspond to 9.6, 16.5, 23.2, 28.9, 38.6, and 57.9 Å.

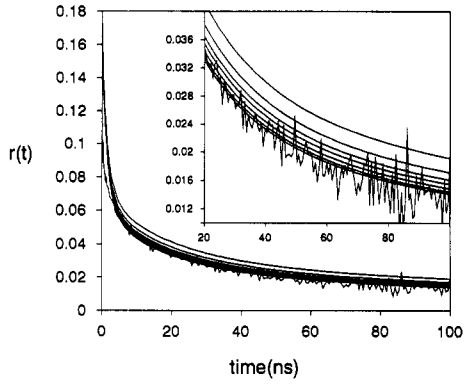

Figure 6. Comparison of experimental time-dependent anisotropy decay for the 20% sample with theoretical calculations based on the model radial distribution function given by eq 4.5. The fastest theoretical decay corresponds to a radial distribution function given by eq 4.4 with σ = 10 Å. Subsequently slower decays correspond to a contact value, σ = 10 Å, and increasing values of the characteristic length, λ, given in Figure 5.

indistinguishable and appear to fit the data best. The agreement is less good for σ = 29.0 Å, although the calculated line still falls within the noise. For σ = 40.5, 46.3, and 57.9 Å, the agreement is poor, indicating a range of contact values that are clearly inconsistent.

The above hard shell analysis reveals the limitations of the resolution in this technique. Apparently, the smallest hard shell distance that can be distinguished from the absence of any excluded volume is on the order of 20 Å. Hard shell effects of this size or larger appear to match the data less well than smaller shells. A finite size shell that is smaller, however, cannot be distinguished in this particular experiment. Therefore, a shell size with $0 < \sigma < 20$ Å is most consistent with this analysis.

As mentioned previously, the physical significance of the contact parameter, σ, can be interpreted as a measure of the cross sectional dimension of the polymer chain. It is reasonable to expect mutually interpenetrating chains to be limited at least by the space taken up by the chains themselves. To estimate the chain cross section, we constructed a molecular model consisting of three methyl methacrylate subunits. According to this model an approximate value of σ = 10 Å was determined.

Figure 5 shows plots of eq 4.5 with σ = 10 Å and λ = 9.6, 16.5, 23.2, 28.9, 38.6, and 57.9 Å. Comparison of the 20% data with calculations based on these radial distributions are shown in Figure 6. The fastest calculated decay corresponds to the radial distribution given by eq 4.4 with σ = 10 Å. Subsequently slower decays correspond to eq 4.5 with increasing values of λ. Similar to the hard shell analysis, increasing the characteristic length leads to progressively poorer agreement with the data. The smallest lengths, λ = 9.6 and 16.5 Å, are distinguishable from the hard shell distribution, although they fall within the noise. Larger values of λ, however, are obviously inconsistent with the data. These comparisons strongly suggest that the form of $g(R_S)$ in this system resembles the most narrow hole distributions shown in Figure 5. Similar to the findings of Honnell et al.,[2] the "correlation hole" must consist primarily of a hard core contact interaction between the chain segments, in this case, about 10 Å.

The limitations in the sensitivity of $r(t)$ to $g(R_S)$ can be understood in terms of the relative contribution to the fluorescence anisotropy from both intra- and intermolecular energy transfer. According to eq 4.2, the anisotropy of the system of interacting tagged polymers contains a multiplicative factor, $r_{on}(t)$, due to the intramolecular EET. Since $r_{on}(t)$ is less than one for all t, a detectable change in $r(t)$ requires a relatively significant change in the factor $\langle G^S_{off}(t,c)\rangle$, describing the concentration-dependent interchain transport. Therefore, a detailed examination of the interchain structure is limited by intramolecular transfer processes that compete with the intermolecular processes we are interested in.

V. Concluding Remarks

The experiments presented above are the first detailed examination of excitation transport in a controlled system of concentrated tagged polymer coils. The system of atactic 6% poly(methyl methacrylate-*co*-2-vinylnaphthalene) in atactic poly(methyl methacrylate) was chosen to study the complicated excitation dynamics due to donor–donor energy transport among interacting molecules in a polymer glass. The experiments were directly compared to a theory[20] which makes use of the truncated cumulant approximation to the transport master equation.[21,22] It has previously been demonstrated that a detailed understanding of excitation transport in isolated finite volume systems can provide a structural probe. EET experiments on chromophore-tagged polymer chains isolated in untagged polymer hosts have provided information on intramolecular polymer structure with Å resolution.[14] In the present work, attention was given to chain to chain transfer processes which are related to the intermolecular polymer structure. Future studies of chain to chain excitation transfer will provide information on the nature of microphase separation and the microscopic dynamics of spinodal decomposition.

The theoretical predictions, based on an ideality approximation of the intramolecular polymer structure, quantitatively reproduce the concentration-dependent energy transport measurements. Our analysis includes the intermolecular radial distribution function, $g(R_S)$. The results suggest that all values of $g(R_S)$ are remarkably close to unity except for $R_S \leq \sigma$ (the segment diameter ~10 Å), for which $g(R_S)$ is zero. Although the limitations of the method prevent the exact determination of $g(R_S)$, the agreement between the theory and data shown in Figure 3 indicates that the cumulant approximation does provide a useful means to model systems of this complexity.

A similar method utilizing EET may provide the sensitivity needed to study $g(R_S)$ in more detail. This could be achieved by eliminating the contribution of the intramolecular excitation transfer from the experimental observable, by labeling the polymer coils with two different types of chromophores. The first type of chromophore is specified a "donor", while the second type is a "trap". A "donor copolymer" containing one donor chromophore

randomly tagged along the length of the chain is required. Similarly, a "trap copolymer" lightly tagged (~4–8%) with trap chromophores randomly located along the chain length is needed. After selective excitation of a donor molecule, the excitation may transfer to a trap but cannot transfer back to the donor. Measurements of the time-dependent donor fluorescence (or trap fluorescence) would contain the necessary information to determine the transfer rates between an excited donor interacting with an ensemble of traps. EET experiments on samples containing both these types of copolymers would eliminate the intramolecular contribution to the energy transport observable. Experimental and theoretical application of this donor–trap method to polymer systems is currently under development.[39]

Acknowledgment. We would like to thank several scientists working in the field of polymer physics for stimulating discussions. They are Dr. John G. Curro, Professor Kenneth S. Schweizer, Professor Curtis W. Frank, Professor Alice Gast, and Professor Hans C. Anderson. This work was supported by the Department of Energy, Office of Basic Energy Sciences (Contract DE-FG03-84ER13251). We would also like to thank the Stanford Center for Materials Research Polymer Thrust Program for additional support and acknowledge an NSF departmental instrumentation grant (No. CHE 88-21737) which provided computer equipment used in the calculations.

References and Notes

(1) Schweizer, K. S.; Curro, J. G. *J. Chem. Phys.* **1992**, *96*, 3211.
(2) Honnell, K. G.; McCoy, J. D.; Curro, J. G.; Schweizer, K. S. *J. Chem. Phys.* **1991**, *94*, 4659.
(3) Torkelson, J. M. *Macromolecules* **1987**, *20*, 1860.
(4) Chang, L. P.; Morawetz, H. *Macromolecules* **1987**, *20*, 428.
(5) Fredrickson, G. H. *Macromolecules* **1986**, *19*, 441.
(6) Mikes, F.; Morawetz, H.; Dennis, K. S. *Macromolecules* **1980**, *13*, 969.
(7) Amrani, F.; Hung, J. M.; Morawetz, H. *Macromolecules* **1980**, *13*, 649.
(8) de Gennes, P.-G. *Scaling Concepts in Polymer Physics*; Cornell University Press: Ithaca, NY, 1979.
(9) Flory, P. J. *J. Macromol. Sci., Phys.* **1976**, *B12(1)*, 1.
(10) Boue, F.; Daoud, M.; Nierlich, M.; Williams, C.; Cotton, J. P.; Farnoux, B.; Jannink, G.; Benoit, H.; Dupplessix, R.; Picot, C. In *International Atomic Agency*; Vienna, 1977; p 563.
(11) Olaj, O. F.; Pelinka, K. H. *Makromol. Chem.* **1976**, *177*, 3413.
(12) de Gennes, P.-G. *J. Phys.* **1970**, *31*, 235.
(13) Flory, P. J. *Principles of Polymer Chemistry*; Cornell University Press: Ithaca, NY, 1953.
(14) Peterson, K. A.; Zimmt, M. B.; Linse, S.; Domingue, R. P.; Fayer, M. D. *Macromolecules* **1987**, *20*, 168.
(15) Ediger, M. D.; Domingue, R. P.; Peterson, K. A.; Fayer, M. D. *Macromolecules* **1985**, *18*, 1182.
(16) Kaplan, D. S. *J. Appl. Polym. Sci.* **1976**, *20*, 2615.
(17) Ediger, M. D.; Domingue, R. P.; Fayer, M. D. *J. Chem. Phys.* **1984**, *80*, 1246.
(18) Peterson, K. A.; Stein, A. D.; Fayer, M. D. *Macromolecules* **1990**, *23*, 111.
(19) Marcus, A. H.; Diachun, N. A.; Fayer, M. D. *J. Phys. Chem.* **1992**, *96*, 8930.
(20) Marcus, A. H.; Fayer, M. D. *J. Chem. Phys.* **1991**, *94*, 5622.
(21) Huber, D. L. *Phys. Rev. B* **1979**, *20*, 2307.
(22) Huber, D. L. *Phys. Rev. B* **1979**, *20*, 5333.
(23) Gochanour, C. R.; Andersen, H. C.; Fayer, M. D. *J. Chem. Phys.* **1979**, *70*, 4254.
(24) Haan, S. W.; Zwanzig, R. J. *J. Chem. Phys.* **1978**, *68*, 1879.
(25) Blumen, A. *J. Chem. Phys.* **1980**, *72*, 2632.
(26) Hoel, P. G.; Port, S. C.; Stone, C. J. *Introduction to Probability Theory*; Houghton-Mifflin: Boston, 1971.
(27) Förster, T. *Ann. Phys.* **1948**, *2*, 55.
(28) Baumann, J.; Fayer, M. D. *J. Chem. Phys.* **1986**, *85*, 4087.
(29) Doi, M.; Edwards, S. F. *The Theory of Polymer Dynamics*; Oxford University Press: Oxford, 1986.
(30) Honnell, K. G.; Curro, J. G.; Schweizer, K. S. *Macromolecules* **1990**, *23*, 3496.
(31) Schweizer, K. S.; Curro, J. G. *J. Chem. Phys.* **1988**, *89*, 3350.
(32) Schweizer, K. S.; Curro, J. G. *J. Chem. Phys.* **1988**, *89*, 3342.
(33) Schweizer, K. S.; Curro, J. G. *Phys. Rev. Lett.* **1987**, *58*, 246.
(34) Curro, J. G.; Schweizer, K. S. *J. Chem. Phys.* **1987**, *87*, 1842.
(35) Curro, J. G.; Schweizer, K. S. *Macromolecules* **1987**, *20*, 1928.
(36) Inokuti, M.; Hirayama, F. *J. Chem. Phys.* **1965**, *43*, 1978.
(37) O'Connor, D. V.; Phillips, D. *Time-correlated single photon counting*; Academic Press: London, 1984.
(38) Schweizer, K. S., private communication.
(39) Marcus, A. H.; Diachun, N. A.; Fayer, M. D., to be published.